In vivo functional photoacoustic micro-imaging of the electrically stimulated rat brain with multi-wavelengths

Lun-De Liao[a], Meng-Lin Li[b], Hsin-Yi Lai[a], You-Yin Chen[a], Paul C.-P. Chao[a]* and Po-Hsun Wang[b]

[a]Department of Electrical Engineering, National Chiao Tung University, Hsinchu 30013, Taiwan.

[b]Department of Electrical Engineering, National Tsing Hua University, Hsinchu, 30013, Taiwan.

*Email: pchao@mail.nctu.edu.tw

ABSTRACT

In this study, we report on using multi-wavelength photoacoustic microscopy to image hemodynamic changes of total hemoglobin concentration (HbT) (i.e., blood volume) and oxygenation (SO_2) in rat brain cortex vessels with electrical stimulation. Electrical stimulation of the rat left forelimb was applied to evoke changes in vascular dynamics of the rat somatosensory cortex. The applied current pulses were with a pulse frequency of 3 Hz, pulse duration of 0.2 ms, and pulse amplitude of 5 mA, respectively. The imaging target of rat brains was demarcated at AP 0 – -2.5 mm and ML ± 6 mm with respect to bregma. HbT changes were probed by images acquired at 570 nm, a hemoglobin isosbestic point while SO_2 changes were imaged by those acquired at 560 nm or 600 nm and their derivatives, which were normalized to those with 570 nm wavelengths. Correlation between the electrical stimulation paradigm and images acquired at 570, 560, and 600 nm in contralateral and ipsilateral vasculature was statistically analyzed, showing that the HbT and SO_2 changes revealed by multi-wavelength photoacoustic images spatially correlated with contralateral vasculature.

Keywords: Functional photoacoustic microscopy, Rat's brain imaging, Electrical stimulation, Hemoglobin concentration.

1. INTRODUCTION

Imaging hemoglobin oxygen saturation (SO_2) changes possesses a crucial role for understanding the brain functions and originating from environmental has a broad range of medical applications as well as monitoring therapeutic interventions of major diseases. Using the imaging techniques to directly image the SO_2 changes are important for disease diagnosis. Functional magnetic resonance imaging (fMRI) and diffusion optical imaging (DOI) can be used to assess changes of oxygenation *in vivo*. Hyder *et al* have been first performed the brain cortical representation during electrical stimulation of the forepaw using fMRI [1]. The relative cerebral blood volume (CBV) during rat forepaw stimulation has also been discussed and found the correlation to the BOLD signals [2]. Keilholz *et al* examined by

Photons Plus Ultrasound: Imaging and Sensing 2010, edited by Alexander A. Oraevsky, Lihong V. Wang,
Proc. of SPIE Vol. 7564, 75643F · © 2010 SPIE · CCC code: 1605-7422/10/$18 · doi: 10.1117/12.843085

comparing the BOLD and CBV-weighted functional imaging for whole-brain fMRI of the rat during forepaw stimulation using the contrast agent dose [3]. However, the fMRI technique is difficult to isolate the contribution from blood volume changes and the DOI offers insufficient spatial resolution to delineate the fine details of a specific brain structures due to strong optical scattering [4]. A better technique for directly SO_2 imaging is needed.

Photoacoustic imaging is a optical-absorption based hybrid imaging technique combining optics and ultrasound. A pulsed laser in the visible or NIR range irradiates a biological sample, and the optical absorption of the biological tissue induces photoacoustic (PA) waves via the thermoelastic effect [5]. With the PA signals detected by highly sensitive ultrasound receivers, the distribution of optical absorptions in the sample can be reconstructed [6]. Photoacoustic imaging possesses high optical absorption contrast of biological tissues instead of low acoustic contrast in ultrasound imaging while its spatial resolution is determined primarily by the ultrasonic characteristics of of generated PA waves rather than by the optical diffusion as in optical imaging [6-7]. By taking advantage of ultrasonic detection, PA imaging can provide better spatial resolution than DOI. In recent years, it has been proved that this technique can assess changes in the concentrations of oxy- and deoxy-hemoglobin [8]. Maslov *et al* proposed a reflection-mode photoacoustic microscopy (PAM) technique that uses dark-field illumination by showing the ability of dark-field functional PAM to track the changes of blood oxygenation in the mouse brain by hypoxic and hyperoxic challenges with multi-wavelengths [9-10]. Stein *et al* have been show the potential of PAM in functional brain SO_2 imaging during the electrically stimulation [11].

In this regard, we established a functional PAM system that can be used to assess the functional changes of SO_2 and CBV in the brain. Electrical forepaw stimulation was employed to activate the contralateral primary somatosensory cortex of forepaw. Correlation between the electrical stimulation paradigm and images acquired at 570, 560, and 600 nm in contralateral and ipsilateral vasculature was statistically analyzed in detail. Our results showed that functional PAM system can robustly image SO_2 and CBV in brain tissues by using intrinsic optical absorptions contrast. This technique has potential to deepen our understanding of brain neurovascular coupling as well as monitor disease progression.

2. MATERIALS AND METHODS

2.1. Experimental animals

Six male Wistar rats (National Laboratory Animal Center, Taiwan) weighing 250-350 grams were used. The animals were housed at a constant temperature and humidity with free access to food and water. Before the imaging experiment, the rats were fasted for 24 hours but given water ad libitum. All animal experiments were conducted in accordance with guidelines from Animal Research Committee of National Chiao-Tung University and National Tsing Hua University.

The animals were initially anesthetized by 3% isoflurane. A PE-50 catheter was inserted in the left femoral vein for subsequent α-chloralose anesthesia (70 mg/kg). The anesthetized rats were mounted on the custom-made acrylic stereotaxic head holder, and the skin and muscle was cut away from the skull to expose the landmark called the bregma.

The anteroposterior (AP) distance between the bregma and the interaural line [12] was directly surveyed. The bregma was 9.3 ± 0.12 mm (mean ± standard deviation) anterior to the interaural line [data not published]. Furthermore, the craniotomy was performed for each animal and the bilateral cranial window with approximately 10 (horizontal) × 8 (vertical) mm size was fashioned with a high-speed drill. After the rat was secured to the stereotaxic frame and placed on the bed pallet, the pallet was moved until the crosshair of the laser alignment system was positioned at the bregma, which was 9 mm anterior to an imaginary line drawn between the centers of each ear bar (the interaural line). The interaural and bregma references were then used to position the heads in the fPAM system without additional surgery in following experiments.

2.2. Functional PA imaging and statistical analysis

After bregma position, the ultrasound C-scan is performed for searching the brain sections for functional images and reference image. It is also used to ensure the scan head was on the focused depth with 12 ± 5 mm below the laser-illumination surface. Following performing the ultrasound C-scan, an image of the brain surface vessels were acquired by the PA C-scan after the laser repetition rate was filed at 10 Hz and tuned to 570 nm wavelength (λ_{570}). Figure 1(A) shows the open-skull anatomical photograph of a prepared rat brain taken prior to all the imaging process. A C-scan data of vasculature of the rat's brain cortex prior to performing functional imaging depicting the 8.5 × 5.5 mm scanned region was imaged *in vivo,* as shown in Figure 1(B). The PA projected C-scan image includes 85 B-scan images with scanning distance apart by 100 μm. As shown in Figure 1(B), cortical blood vessels indicated by the solid arrows in Figure 1(A) are imaged. In addition, some branches of these vessels are also visualized in the projected C-scan image.

Then, a pair of needle electrodes was inserted under the skin of rat's left forepaw. The electrical stimulation of left forepaw was applied using the electrical stimulator (Model 2100, A-M Systems, U.S.A) with a monophasic constant current of 3 Hz frequency. The pulse duration was 0.2 ms with the intensity of 5 mA. Reference images ($I_{R(570)}$) at λ_{570} with stimulus-OFF ($I_{R\,(570),\,stimulation\text{-}OFF}$) and stimulus-ON ($I_{R(570),\,stimulation\text{-}ON}$) paradigm and images ($I$) for the same region at λ_{560} or λ_{600} with stimulus-OFF ($I_{(560\ or\ 600),\,stimulation\text{-}OFF}$) and stimulus-ON ($I_{(560\ or\ 600),\,stimulation\text{-}ON}$) paradigm were acquired.

The functional images ($\Delta I_{F(560\ or\ 600)}$) were then constructed according to the following equation:

$$\Delta I_{F(560\ or\ 600)} = \frac{I_{(560\ or\ 600\ \mathrm{nm})stimulation-ON}}{I_{R(570\ \mathrm{nm})stimulation-ON}} - \frac{I_{(560\ or\ 600\ \mathrm{nm})stimulation-OFF}}{I_{R(570\ \mathrm{nm})stimulation-OFF}}$$
$$= I_{F(560)stimulation-ON} - I_{F(560)stimulation-OFF} \quad (1)$$

In the current fPAM system, data acquisition time for a PA B-scan image with 135 scanlines (8 mm width) is about 14 seconds. That is, it takes about 56 seconds for one functional image of $\Delta I_{F(560\ or\ 600)}$. For one given brain section, the same functional imaging procedure will be repeated for three times.Three functional images at bregma +1 mm,-1.5 mm and -2.5 mm in response to left forepaw stimulation were acquired to identify changes in PA signal. For accurately

deciding region of interests (ROIs) of the PA changes in coronal brain slices, a modified laboratory-built ISPMER imaging processing system [13] was performed the fusion of PA images and rat brain atlas to define the anatomical borderlines of primary somatosensory cortex of forepaw (S1FL) from brain section at bregma +1 mm and -1.5 mm and somatosensory cortex of the trunk (S1Tr) area from a brain section at bregma -2.5 mm, respectively.

The experiment was designed to quantitatively compare the differences in PA signal changes in bilateral brain structures resulting from stimulation of the left forepaw of the rat. The ROIs in the cortical areas of S1FL and S1Tr, which are clearly bilateral structures, were examined for side-to-side differences in PA signals using a paired *t*-test ($p < 0.05$). Differences in activation were tested between two conditions of stimulus-OFF and stimulus-ON for each ROI. Repeated-measures analysis of variance (ANOVA) ($n = 3$) was applied for multiple comparisons with Bonferroni correction. All statistical analyses were performed using SPSS (version 10.0, SPSS®, U.S.A) for Windows (version 2002, Microsoft Windows XP®, U.S.A).

3. RESULTS

3.1. $I_{R(570)}$ *imaging of the blood vessels distribution in cerebral cortex*

The open-skull window of the rat cortical surface was shown in Figure 1(A). Many blood vessels in this surface can be observed. We can visually observe the superior sagittal sinus (SSS) and other big vessels on the cortical surface indicated by the red solid arrows in Figure 1(A) and 1(B). The vasculature of the rat brain cortex in the open window was imaged *in vivo* by fPAM at λ_{570}, which is shown in Figure 3(B). As shown in Figure 1(B), cortical blood vessels indicated by the solid arrows in Figure 1(A) are imaged. In addition, some branches of these vessels are also visualized in the projected C-scan image. However, it is noted that SSS was not well imaged by the current fPAM system, which is similar to the result obtained in reference [10]. Geometric focusing and finite detection bandwidth of the used ultrasound transducer may account for the weakness of the detected PA signals from SSS.

3.2. $I_{R(570)}$ *PA signal changes in the bilateral brain region under stimulus-OFF and stimulus-ON conditions*

Quantitative analysis showed that the significant functional changes of $I_{R(570)}$ in the corresponding to the contralateral S1FL regions at bregma +1 mm,-1.5 mm and S1Tr at bregma -2.5 mm were detected about 3.58 %, 3.45 % and 3.51 %, respectively, as shown in Figure 2 ($p < 0.05$; stimulus-OFF and stimulus-ON). Moreover, no significant bilateral difference (about 0.78 %, 0.65 % and 0.89 %) under the stimulus-OFF condition were detected in the contralateral S1FL regions located at bregma +1 mm, -1.5 mm and S1Tr at bregma -2.5 mm ($p > 0.05$; paired *t*-test), respectively. In addition, the bilateral difference in the S1FL regions at bregma +1 mm and bregma -1.5 mm and S1Tr at bregma -2.5 mm detected under stimulus-ON are about 3.12 %, 2.93 % and 3.23 %, which is significant ($p < 0.05$; paired *t*-test).

3.3. $I_{F(560)}$ or $I_{F(600)}$ *PA signal changes in the bilateral brain region under stimulus-OFF and stimulus-ON conditions*

Quantitative analysis of the $I_{F(600)}$ PA signals in the contralateral S1FL region at bregma +1 mm is decreased about 4.56 % under the stimulation-ON, as shown in Figure 3(A). Contrariwise, the $I_{F(600)}$ PA signals in the contralateral S1FL region at bregma -1.5 mm and S1Tr region at bregma -2.5 mm sections are increased about 2.23 % and 2.8 % under the stimulation-ON, respectively ($p < 0.05$; paired *t*-test). In addition, the $I_{F(600)}$ PA signals are decrease about 4.18% in contralateral S1FL region at bregma +1 mm under the stimulation-ON, as shown in Figure 3(B). ($p < 0.05$; paired *t*-test). The $I_{F(600)}$ PA signals in the contralateral S1FL region at bregma -1.5 mm and in the contralateral S1Tr region at bregma -2.5 mm are increased about 2.21% and 2.37 % under the stimulation, respectively ($p < 0.05$; paired *t*-test), as shown in Figure 3(B). Moreover, both of $I_{F(560)}$ and $I_{F(600)}$ PA signals are no bilateral difference under the stimulation-OFF. The lateralized difference in cortical contralateral S1FL at bregma +1, -1.5 mm and S1Tr at bregma -2.5 mm were significant under the stimulation-ON ($p < 0.05$, paired *t*-test). The results show that the $I_{F(560)}$ and $I_{F(600)}$ PA signals changes are inverse proportion to the changes of SO_2. It is also noted that the absorption ratio of λ_{560} is higher than λ_{600}. Therefore, the changes of $I_{F(560)}$ will be a little bit higher than $I_{F(600)}$ [14].

4. CONCLUSION

The results showing that the functional PA signals acquired at 560 or 600 nm are inverse proportion to the SO_2 changes during the electrical stimulation. That is, functional PA signals decreases when the SO_2 changes increases. This phenomenon correlated well with the previous PAM and MRI studies [10,15]. In summary, the current fPAM system was successfully established for detecting the brain PA signals in response to changes in neuronal activities induced by forepaw electrical stimulation. The present study demonstrated that fPAM system is able to provide novel SO_2 and CBV mapping in a single setting. *In vivo* measurement of brain hemodynamics with a radiation-free, intrinsic contrast of optical absorptions becomes reality.

ACKNOWLEDGMENTS

The authors are greatly indebted to the National Science council of R.O.C. for the support of the research through contact in Nos. NSC 96-2220-E-009-029, and NSC 97-2221-E-007-084-MY3.

FIGURES

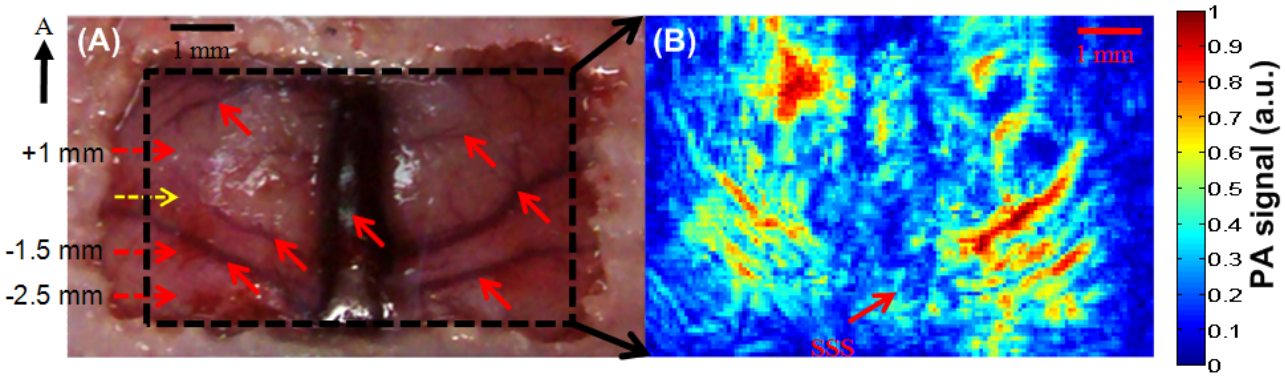

Figure 1. Comparison of the open-skull photograph with $I_{R(570)}$ PA C-scan image. The black crossed arrow points in the rostra direction both figures. (A) Open-skull photograph of the rat's brain surface. The yellow dashed line indicates the PA image through the bregma as a reference image. Functional B-scan image obtained from scanning along the red dashed lines relative to reference image at +1 ,-1.5, and -2.5 mm, respectively. The red arrowheads indicate that the brain cortex vessels, as shown in Figure 1(A). (B) *In vivo* $I_{R(570)}$ PA C-scan image of the blood vessels in the superficial layer of the cortex. The vascular patent has been imaged by the $I_{R(570)}$ PA C-scan image. Comparing with the red arrowheads indicated in (A), the capillaries nearby the vessels were clearer imaged. Not that the redder areas indicate greater optical absorption.

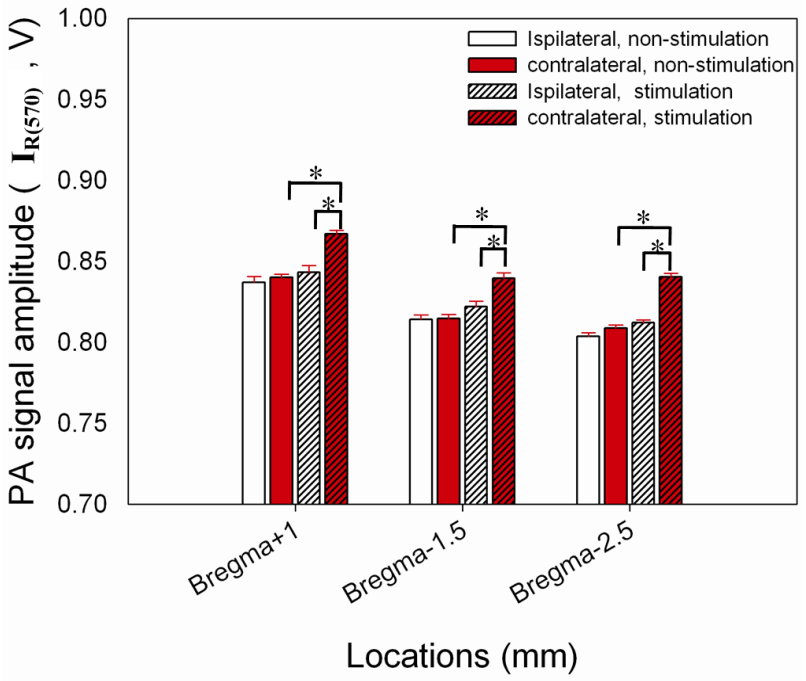

Figure 2. Statistical analysis of the $I_{R(570)}$ PA signals changes in the bilateral regions between the stimulation-ON/OFF conditions and the bilateral difference under the stimulation for the bilateral regions in primary somatosensory cortex of forepaw (S1FL) from brain section at bregma +1 mm and -1.5 mm, and somatosensory cortex of the trunk (S1Tr) area at bregma -2.5 mm, respectively. The results revealed that the $I_{R(570)}$ PA signal with significant changes in the contralateral interested regions under stimulation-ON. * denotes significant differences ($p < 0.05$; paired t-test).

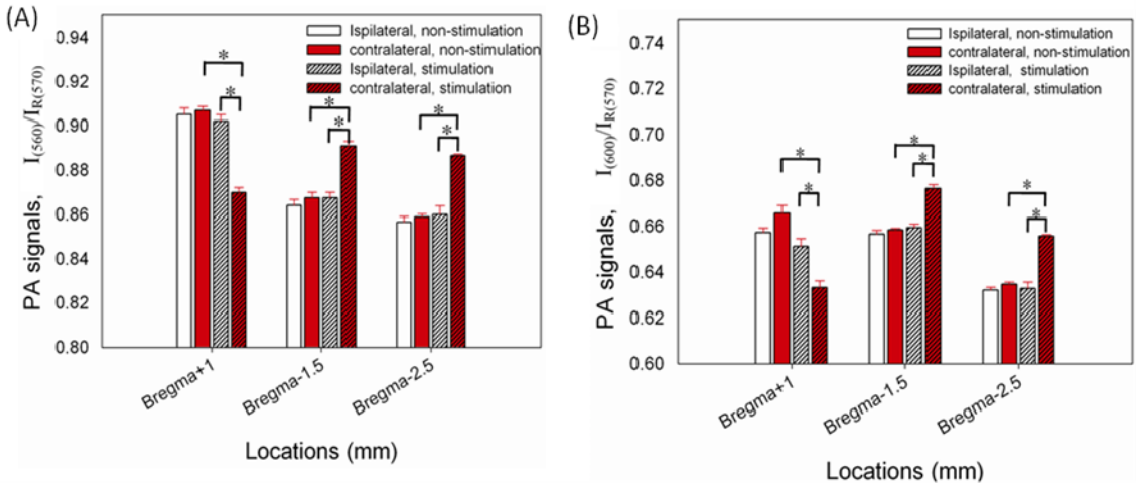

Figure 3. Quantitative analysis of the $I_{F(560\ or\ 600)}$ PA signals in the bilateral regions between the stimulation-ON/OFF conditions and the bilateral difference under the stimulation-ON. The differences between the stimulation-ON/OFF and lateralizes phenomenon under the stimulation-ON are significant. * denotes significant differences ($p < 0.05$; paired t-test).

REFERENCES

[1] Hyder F., Behar K. L., Martin M. A., Blamire A. M., and Shulman R. G., "Dynamic magnetic resonance imaging of the rat brain during forepaw stimulation," Journal of Cerebral Blood Flow and Metabolism 14 (4), 649-655 (1994).

[2] Mandeville J. B., Marota J. J. A., Kosofsky B. E., Keltner J. R., Weissleder R., Rosen B. R., and Robert M. W., "Dynamic functional imaging of relative cerebral blood volume during rat forepaw stimulation," Magnetic Resonance in Medicine 39 (4), 615-624 (2005).

[3] Keilholz S.D., Silva A.C., Raman M., Merkle H., and Koretsky A.P., "BOLD and CBV-weighted functional magnetic resonance imaging of the rat somatosensory system," Magnetic Resonance in Medicine 55, 316-324 (2006).

[4] Wang L. V. and Wu H.-i, *Biomedical Optics: Principles and Imaging*. (Wiley, 2007); Gabriele Gratton and Monica Fabiani, "Dynamic brain imaging: event-related optical signals (EROS) measures of the time course and localization of cognitive-related activity," Psychonomic Bulletin & Review 5 (4), 535-563 (1998).

[5] Wang L. V., *Photoacoustic Imaging and Spectroscopy*. (CRC, 2009).

[6] Wang L. V., "Tutorial on Photoacoustic Microscopy and Computed Tomography," IEEE Journal of Selected Topics in Quantum Electronics 14 (1), 171-179 (2008).

[7] Wang L. V., "Multiscale photoacoustic microscopy and computed tomography," Nature Photonics 3 (503-509) (2009).

[8] Fainchtein R., Stoyanov B. J., Murphy J. C., Wilson D. A., and Hanley D. F., "Local determination of hemoglobin concentration and degree of oxygenation in tissue by pulsed photoacoustic spectroscopy," Proc. SPIE 3916, 19-33 (2000).

[9] Maslov K., Stoica G., and Wang L. V., "In vivo dark-field reflection-mode photoacoustic microscopy," Optics Letter 30 (6), 625-627 (2005).

[10] Stein E. W., Maslov K., and Wang L. V., "Noninvasive, in vivo imaging of blood-oxygenation dynamics within the mouse brain using photoacoustic microscopy," Journal for Biomedical Optics 14 (2), 020502 (2009).

[11] Stein E. W., Maslov K., and Wang L. V., "Noninvasive mapping of the electrically stimulated mouse brain using photoacoustic microscopy " Proceedings of SPIE 6856 (68561J) (2008).

[12] Paxinos G., Watson C., *The rat brain in stereotaxic coordinates*. (Academic Pr, 2007).

[13] Shih Y.-Y., Chen Y.-Y., Chen J.-C., Chang C., and Jaw F.-S., "ISPMER: Integrated system for combined PET, MRI, and electrophysiological recording in somatosensory studies in rats," Nuclear Instruments and Methods in Physics Research A 580, 938-943 (2007).

[14] "Optical Spectra, Oregon Medical Laser Center".

[15] Sanganahalli B. G., Herman P., and Hyder F., "Frequency-dependent tactile responses in rat brain measured by functional MRI," NMR in Biomedicine 21, 410-416 (2008).